Proceedings of the 28th IEEE
EMBS Annual International Conference
New York City, USA, Aug 30-Sept 3, 2006

Registering fNIR Data to Brain Surface Image using MRI templates

Hasan Ayaz, Meltem Izzetoglu, Steven M. Platek, Scott Bunce, Kurtulus Izzetoglu, Kambiz Pourrezaei and Banu Onaral, *Fellow, IEEE*

Abstract— **Functional near-infrared spectroscopy (fNIR) measures changes in the relative levels of oxygenated and deoxygenated hemoglobin and has increasingly been used to assess neural functioning in the brain. In addition to the ongoing technological developments, investigators have also been conducting studies on functional mapping and refinement of data analytic strategies in order to better understand the relationship between the fNIR signal and brain activity. However, since fNIR is a relatively new functional brain imaging modality as compared to positron emission tomography (PET) and functional magnetic resonance imaging (fMRI), it still lacks brain-mapping tools designed to allow researchers and clinicians to easily interact with their data. The aim of this study is to develop a registration technique for the fNIR measurements using anatomical landmarks and structural magnetic resonance imaging (MRI) templates in order to visualize the brain activation when and where it happens. The proposed registration technique utilizes chain-code algorithm and depicts activations over respective locations based on sensor geometry. Furthermore, registered data locations have been used to create spatiotemporal visualization of fNIR measurements.**

I. Introduction

THERE has been a recent increase in the utilization of functional near infrared spectroscopy (fNIR) which is an emerging neuroimaging modality. Its unique attributes such as being relatively inexpensive, safe, portable, noninvasive and nonintrusive allow its utilization in key areas such as neurohabilitation, learning, mental health, sports medicine, pediatric and emergency medicine.

fNIR spectroscopy uses light in the near-infrared range (700-900nm) to monitor changes in the concentrations of oxygenated hemoglobin (oxy-Hb) and deoxygenated hemoglobin (deoxy-Hb). [1-4]. Biological tissues are mostly transparent to near infrared light in the range of 700 to 900nm wavelength. Fortunately, deoxy- and oxy-hemoglobin have distinctive absorption characteristics which allow one to determine changes in their concentrations using incident light at specific wavelengths together with the modified Beer Lambert law [1,2,5].

fNIR is used to detect cognitive activity related to a stimuli by comparing oxygenation and blood volume changes before and after the presentation of the stimuli. Cognitive activity is determined with respect to cerebral hemodynamic response since cerebral hemodynamic changes are related to functional brain activity through a mechanism which is called neurovascular coupling [2,3].

Optical techniques have been applied to the study of brain oxygenation and metabolism for several decades [6]. Noninvasive monitoring of human brain function by fNIR has been extensively studied in recent years for various types of brain activity including motor [7,8], visual [4], auditory [9], olfactory [10], speech recognition [11], face recognition [12] and even higher cognitive tasks [13,14]. A recent review about fNIRS can be obtained from Gratton et al. [15] and Izzetoglu et al [16].

This growing focus on fNIR experimentation urges development of data visualization and registration techniques for comparison and analysis purposes. This challenge has been recognized and a group of studies started to address it [17, 19, 20]. Unfortunately, fNIR data is not acquired with a structural brain image like fMRI, spatial data locations are strictly related to source-detector geometry and although light source and detectors that collect data are on the head surface, data itself is related to the changes in the concentrations of oxy-Hb and deoxy-Hb in the cortex. These issues are the main road-blocks for a universal fNIR data registration scheme.

In this study, we developed registration and visualization schemes for fNIR data where the activation patterns in the cortex can be visualized on their corresponding locations on brain surface images. Here, the algorithms are applied to a 16 voxel (volumetric pixel) fNIR sensor geometry

Manuscript received April 24, 2006. This work has been sponsored in part by funds from the Defense Advanced Research Projects Agency (DARPA) Augmented Cognition Program, the Office of Naval Research (ONR) and Department of Homeland Security (DHS), under agreement numbers N00014-02-1-0524, N00014-01-1-0986 and N00014-04-1-0119

B. Onaral, K. Pourrezaei, K. Izzetoglu, M. Izzetoglu and H. Ayaz are with the Drexel University, School of Biomedical Engineering, Science and Health Systems, Philadelphia PA 19104 USA (Direct correspondence to; phone: 215 895 1988; fax: 215 905 4983; e-mail: ayaz@ drexel.edu).

S. M. Platek, is with Department of Psychology, Drexel University, Philadelphia, PA 19104.

S. Bunce is with the Department of Psychiatry, Drexel University College of Medicine, Philadelphia, PA 19102.

designed to collect data from the pre-frontal cortex. We have used front, left and right view of frontal lobe brain surface images obtained from the Digital Anatomist Project, conducted by department of Biological Structure, University of Washington.

II. fNIR Sensor and Measurement Locations

Figure 1 below depicts the fNIR sensor pad that has been designed for forehead. Within this schema, corresponding source detector distance is 25mm. All light sources and detectors form a rectangular grid and positioned on the head surface. The probe is made of flexible circuit board that fits the forehead curvature.

Light that reaches the detector follows a banana shaped path originating from the corresponding light source [4,8]. Measurement point or volumetric pixel (voxel) of interest that reaches down the cortex is at the ridge of this banana shaped path. Therefore, voxel locations are in the middle between the light source and detector.

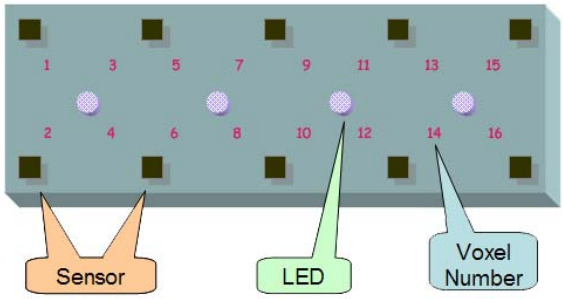

Fig. 1. Voxel locations and geometry of fNIR Probe. All 16 voxels are in a rectangular grid and are in between light source and sensor.

During measurements, probe is placed on the forehead so that the horizontal symmetry axis (central y-axis) coincides with symmetry axis of the head, i.e. in between the eyes. On the vertical axis, sensor is positioned with respect to international 10-20 head marker system (Homan, et al 1987). Fp1 and Fp2 marker locations are positioned on the bottom 'voxel row' level.

III. METHODS

The main objective in this study is to register the voxel locations onto the frontal lobe brain surface image and visualize them from front, right and left views. This would allow the researchers and clinicians to compare experimental results, view the activation regions and to interpret the overall fNIR data. The assumption in the mapping and visualization techniques developed is that brain structure approximately follows the curvature of the forehead as does the sensor, that is cortex-to-scalp distance is constant throughout forehead. The study by Knecht et al. [28] has found through MRI that cortex-to-scalp distance changes throughout head. However, this variability can be insignificant over certain homogenous regions. In our case, we are interested in the forehead and assume the cortex-to-scalp distance is constant in this region.

A. Mapping

The term mapping is used here to define the concept of registration of the fNIR data that has been collected using the probe structure shown in Figure 1 on to 2D brain surface images.

The proposed mapping technique is consisted of 5 steps.

Step 1: Identification of the reference points on the brain surface image.

The mapping of the fNIR data is performed on standardized MRI templates of SPM2 obtained from 152 subject structural MRI image averages. Okamoto, et al [18] had provided the relationship between head and cortex surfaces and standardized brain template by marking the international 10-20 system head locations on both surfaces within structural MRI images. Using these head locations as reference points, the vertical locations of the fNIR data is mapped on to 2D brain surface image. While performing the mapping, vertical locations are transformed taking into account the size (height and width) of the standardized brain template. The horizontal locations are found after performing the following steps.

Step 2: Calculation of the curvature of the forehead in the transverse plane and removal of the unwanted skull area

An MRI slice that corresponds to the bottom row of voxels is shown in Figure 2. The curvature information of the brain surface and the skull is extracted by first thresholding the MRI slice. The threshold of the gray-scale

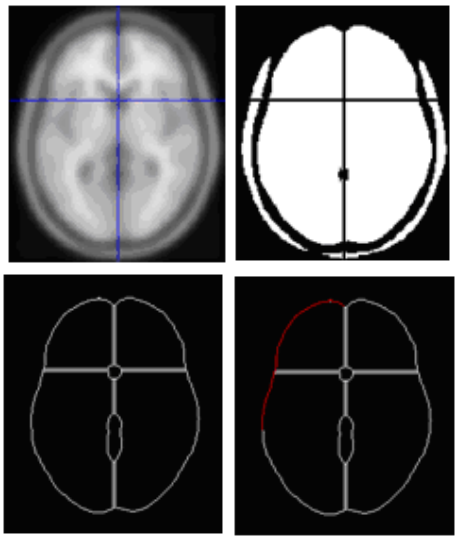

Fig. 2. Steps of calculating forehead chain-code from MRI slice of SPM2 T1 template (Institute of Neurology, University of College London). Slice image is first thresholded & binarized, morphological size filtered, edge detection is applied and finally chain code is extracted.

image is selected as 110 over [0-255] gray pixel scale. Then, pixels that have intensity values greater than the threshold are set to 1 and the remaining ones are taken as background and set to 0. The thresholded and binarized image is shown in Figure 2 step 2.

The unwanted skull area in our measurement region, is removed using a morphological size filter. In this operation, connected components in the thresholded and binarized image are first labeled such that white pixel islands in the black background are generated. The number of pixels in each island is then counted and only the four largest islands are selected. Since the islands that correspond to skull are smaller than brain, the unwanted skull area gets eliminated as shown in Figure 2-step 2.

Step 3: Extraction of the surface information

The surface information is extracted by applying edge detection algorithm. Since the image is binary, 3x3 Sobel kernel, [1 2 1; 0 0 0;-1 -2 -1] (for horizontal) and [-1 0 1; -2 0 2;-1 0 1] (for vertical) , is convolved with the image and two convolutions are normalized and added together to create the edge image as shown in Figure 2 step 3.

Step 4: Chain code generation

Chain code is a relative representation of neighboring pixels. The algorithm is essentially an edge tracer which starts with an initial seed and searches the 8 neighbor pixels in clock-wise direction for the same valued one as the initial seed which is 1 in our case. The neighbor pixels to the initial seed pixel are numbered or coded such that south is 1, south-west is 2, west is 3 and so on. Once the neighbor that has white value (1) is found, then the label of it is changed to seed for the next iteration and its code number is recorded. The algorithm tracks the border line by repeating this procedure until the pixel that has no neighbor having white value is reached. Algorithm has a one-back memory and paints the pixels that have been passed through to red to make sure it follows the right direction.

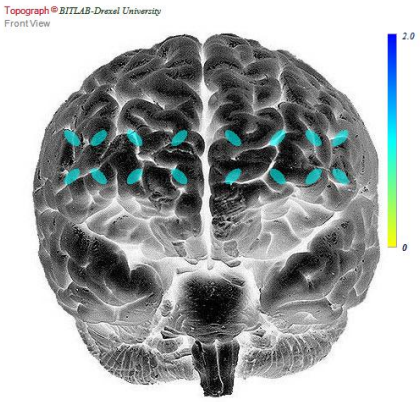

Fig. 3. Registered 16 voxel locations depicted as with ellipses on the inverted brain surface image.

Step 5; Projection of curved 3D head voxel locations onto 2D brain surface image

Since voxel locations are fixed/known on the 3D sensor geometry, projections on 2D surface image are found by walking through the chain code relative to horizontal symmetry axis. Registered voxel locations are shown in Figure 3.

B. Visualization

In order to visualize the data, we have developed spatial graphs registered on the brain surface image using the mapped voxel locations. These spatial graphs are formed as color coded surfaces by interpolating the intermediate points based on the sensor geometry and thresholding. We have employed common interpolation methods used in medical imaging including: Nearest neighbor, linear, cosine, cubic convolution (2 and 4 point), B-Spline (3rd order), Blackman-Harris windowed sinc (6 point) and Gaussian (2 and 4 point) [21-27]. Figure 4, below, has front, right and left views of a spatial graph obtained by using 3rd order BSpline interpolation [22-24].

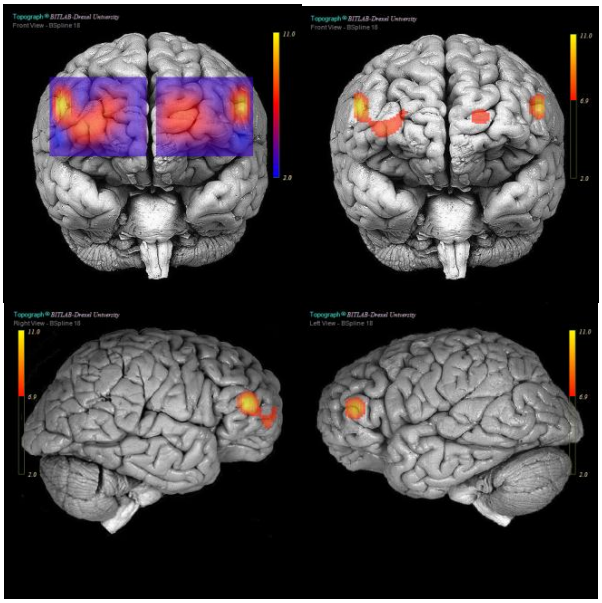

Fig. 4. Spatial graph, registered on the forehead front view, thresholded (with 138 over 255) and right and left views respectively.

We have also developed real-time videos that reflect activation patterns within the same time scale that they are recorded. These videos are compiled from frames by rendering these registered spatial graphs for spatiotemporal visualization and allowed us to better interpret the responses to a stimulus and compare inter-intra subject activity patterns.

Let us note here that Figure 3 represents the true information on the oxy/deoxy concentrations since those are the original data points measured by the fNIR sensor. Figure 4, on the other hand, is a mathematical extrapolation

of the true measurement points onto the entire forehead area spanned by the fNIR sensor pad. In this representation, the interpolated data in between voxels may not be biologically accurate - i.e., oxygenation may change across a sulcus, and the mathematical model would not take this into account unless it was centered over a voxel. Therefore, interpolated spatial maps cannot be held to be a veridical representation of underlying brain function which is true only at the voxel centroids. Whereas spatiotemporal visualization using spatial maps can provide a better understanding of the localization and progress of oxygenation changes, given the heterogeneity of the prefrontal cortex, any interpretation of the areas between voxels must be made with caution.

IV. Conclusion

fNIR is a promising brain monitoring modality which has gained recent interest from researchers and clinicians because of its unique characteristics. A universal visualization technique is required to compare fNIR data within and across subjects and with other modalities such as fMRI and PET. In this study we have presented a method to register and visualize fNIR data on brain surface. Currently, we are working on further developments in the algorithm such as exploration of its applicability to different fNIR sensor geometries and assembly of the tool in a software package.

References

[1] Chance, B., Zhuang Z., UnAh, Z., Alter C, Lipton, L., (1993) "Cognition-activated low-frequency modulation of light absorption in human brain",PNAS 90: 3770-3774

[2] Chance B., Anday E., Nioka S., Zhou S., Hong L., Worden K., Li C., Murray T., Ovetsky Y., Pidikiti D., Thomas R.,(1998) A novel method for fast imaging of brain function, non-invasively, with light, Optics Express, Vol 2, No. 10, 411

[3] Villringer, A., Planck, J., Hock, C., Schleinkofer, L., & Dirnagl, U.,(1993) "Near infrared spectroscopy (NIRS): A new tool to study hemodynamic changes during activation of brain function in human adults". Neuroscience Letters, , 154, 101–104

[4] Villringer, A., Chance, B., 1997 "Non-invasive optical spectroscopy and imaging of human brain function", Trends Neuroscience ,20, 435–442

[5] Chance B., (1951) "Rapid and sensitive spectrophotometry. III. A double beam apparatus," Rev. Scient. Instrum. Vol. 22, pp. 634–638.

[6] Jobsis, F. F. (1977) "Noninvasive, infrared monitoring of cerebral and myocardial oxygen sufficiency and circulatory parameters", Science, 198: 1264-1267

[7] Obrig, H., Hirth, C., Junge-Hulsing, J.G., Doge, C., Wolf, T., Dirnagl, U., Villringer, A., (1996). Cerebral oxygenation changes in response to motor stimulation. J. Appl. Physiol. 81, 1174–1183.

[8] Strangman, G., Boas, D.A., Sutton, J.P., (2002) ,"Non-invasive neuroimaging using near-infrared light", Biological Psychiatry, 2002. 52(7), 679-93..

[9] Sakatani, K., Chen, S., Lichty, W., Zuo, H., & Wang Y. P., (1999) Cerebral blood oxygenation changes induced by auditory stimulation in newborn infants, Early Hum. Dev. 55(3), 229–236

[10] Bartocci M.,Winberg J., Ruggiero C., Bergqvist L. L., Serra G., & Lagercrantz H., (2000) "Activation of olfactory cortex in newborn infants after odor stimulation: a functional near-infrared spectroscopy study," Pediatr Res 48, 18-23.

[11] Sato, H., Takeuchi, T., Sakai, K.., (1999), "Temporal cortex activation during speech recognition: an optical study" Cognition (73), B55-B66

[12] Csibra G., Henty J., Volein A., Elwell C., Tucker L., Meek J., Johnson M. H., (2004) Near infrared spectroscopy reveals neural activation during face perception in infants and adults, J Pediatr Neurol 2004; 2(2): 85-89

[13] Hoshi Y., Onoe H., Watanabe Y., Andersson J., Bergstrom M., Lilja A., Langstom B., & Tamura M., (1994), Non-synchronous behavior of neuronal activity, oxidative metabolism and blood supply during mental tasks in man, Neurosci. Lett. 172, 129-133.

[14] Izzetoglu K, Bunce S, Onaral B, Pourrezaei K, Chance B, (2004). Functional Optical Brain Imaging Using Near-Infrared During Cognitive Tasks. Int. J. of Human-Comp. Int., 17(2):211-227.

[15] Gratton E., Toronov V., Wolf U., Wolf, M., Webb A., (2005) Measurement of brain activity by near-infrared light, Journal of Biomedical Optics, 10(1), 011008

[16] Izzetoglu M, Izzetoglu K, Bunce S, Ayaz H., Deveraj A., Onaral B, Pourrezaei K, (2005). Functional Near-Infrared Neuroimaging. IEEE Trans. on Neural Systems and Rehabilitation Engineering, 13(2):153-159.

[17] Okamoto M., Dan H., Shimuzu K., Takeo K., Amita T., Oda I., Konishi I., Sakamoto K., Isobe S., Suzuki T., Koyama K., & Dan I., (2004), "Multimodal assessment of cortical activation during apple peeling by NIRS and fMRI", NeuroImage, 21, 1275-1288.

[18] Okamoto M., Dan, H., Sakamoto, K., Takeo, K., Shimizu, K., Kohno, S., Oda, I., Isobe, S., Suzuki, T., Kohyama, K., Dan, I., "Three-dimensional probabilistic anatomical cranio-cerebral correlation via the international 10–20 system oriented for transcranial functional brain mapping", NeuroImage 2004, 21, 99–111

[19] Okamoto M., & Dan I., (2005), "Automated cortical projection of head-surface locations for transcranial functional brain mapping" NeuroImage, 26, 18-28.

[20] Singh A., Okamoto M., Dan H., Jurcak V., & Dan I., (2005), "Spatial registration of multichannel multi-subject fNIRS data to MNI space without MRI", NeuroImage, 27, 842 – 851.

[21] Lehman, T. M., Gonner C., Spitzer, K., (1999) "Survey: Interpolation Methods in Medical Image Processing", IEEE Transactions on Medical Imaging, vol. 18, no. 11

[22] Unser M., (1999) "Splines, A perfect fit for signal and image processing", IEEE Signal Processing Magazine, 22-38

[23] Unser, M., Aldroubi, A., Eden, M., (1993) "B-Spline Signal Processing: Part I – Theory", IEEE Transactions on Signal Processing, Vol 41. No. 2 p821-833

[24] Unser, M., Aldroubi, A., Eden, M., (1993) "B-Spline Signal Processing: Part II – Efficient Design and Applications", IEEE Transactions on Signal Processing, Vol 41. No. 2 p834-848

[25] Maeland, E., (1988) "On the Comparison of Interpolation Methods", IEEE Transactions on Medical Imaging, vol. 7, no. 3, pp. 213-217

[26] Thevenaz, P., Blu, T., Unser, M.,(2000) "Interpolation Revisited", IEEE Transactions on Medical Imaging, Vol. 19, No. 7

[27] Meijering, E., Unser, M., (2003) "A note on Cubic Convolution", IEEE Transactions on Image Processing, vol. 12, no. 4, pp. 477–479

[28] Knecht S., Sommer J., Deppe M., Steinstrater O., (2005)," Scalp position and efficacy of transcranial magnetic stimulation", Clinical Neurophysiology 116, 1988–1993.